Thin Solid Films 330 (1998) 34–45

Transport processes in porous media: diffusion in zeolites

Reinhold Haberlandt*

University Leipzig, Institute for Theoretical Physics, Department of Dynamic/Computer Simulations, Augustusplatz 10-11, D-04109 Leipzig, Germany

Abstract

Diffusion of guest molecules (CH_4, C_2H_6, Xe) in zeolites (LTA-zeolites, silicalite) will be discussed under different thermodynamic conditions for different intermolecular potentials. The macroscopic properties will be related to microscopic data using methods of statistical physics and computer simulations (MD, NEMD). Comparisons with PFCI-NMR measurements are given.

Keywords: Zeolites; Diffusion process; Pulsed field gradient nuclear magnetic resonance; Computer simulation

1. Introduction

Zeolites are highly porous media consisting of crystals containing different cavities or channels connected by *windows* (e.g. eight-membered oxygen rings in A-zeolites) or *intersections* in silicalites built up by oxygen, aluminium, silicon and exchangeable cations (sodium, calcium) with very different kind of lattices [1,2]. The size of the pores relative to the diameter of the diffusing molecules is the essential quantity for the diffusion behaviour. More and more zeolites play an important role as well in understanding the structural, thermodynamical and dynamical properties of molecules in confined geometries as in applying in different fields, e.g. as detergents, catalysts and ion-exchangers.

Kärger and Ruthven [3] published an excellent book reviewing the methods to investigate diffusion processes in microporous media, especially in zeolites, and discussing their different experimental results up to three orders of magnitude [3].

Statistical physics and computer simulations [4–7] are valuable tools in researching first the structural and thermodynamical properties (for a review see [8]). Since the paper by Yashonath et al. [9], several groups started also the investigation of diffusion processes in zeolites using computer simulations. More detailed information is available in the literature [10–17]. Two papers reviewing this field were recently published [8,18].

Due to the different structures of the zeolites and depending on the size of the guest molecules the pattern of the dependency of diffusivity on the mean number of guest molecules (loading) is different [3,19].

The aim of the present paper is to summarize our recent results, potential surfaces, density distributions, propagators, diffusion coefficients [20–31] in understanding the diffusion of some special guest molecules in different zeolites in microscopic detail using molecular dynamical simulations (MD) and to compare the evaluated data with measured data [19,28].

Starting with calculations for CH_4 guest molecules in NaCaA and its cation-free analogue (for short, not quite exact: ZK4), additionally C_2H_6 in ZK4 is taken into account. As another example the diffusion of guest molecules (C_2H_6 and a mixture of CH_4, Xe, respectively) in silicalite is considered.

The structure of the LTA type zeolite is demonstrated in Fig. 1. It shows (left) the general structure of zeolites of type LTA used for the calculations. The sodalite units form a cubic lattice with large cavities connected by so-called *windows* consisting of eight oxygen atoms. In Fig. 1 (right) the distribution of the lattice atoms around a large cavity in the NaCaA zeolite is to be seen. Lattice atoms in front have been removed in order to see the interior of the cavity. Windows are marked by a small *w*.

While the guest molecules move via windows from one to the other large cavity in LTA zeolites, in the silicalites they migrate through straight and so-called *zig-zag* channels from intersection to intersection [1–3].

* Tel.: +49 341 2352280; fax: +49 341 2352307;
e-mail: reinhold.haberlandt@physik.uni-leipzig.de

0040-6090/98/$ - see front matter
PII S0040-6090(98)00798-6

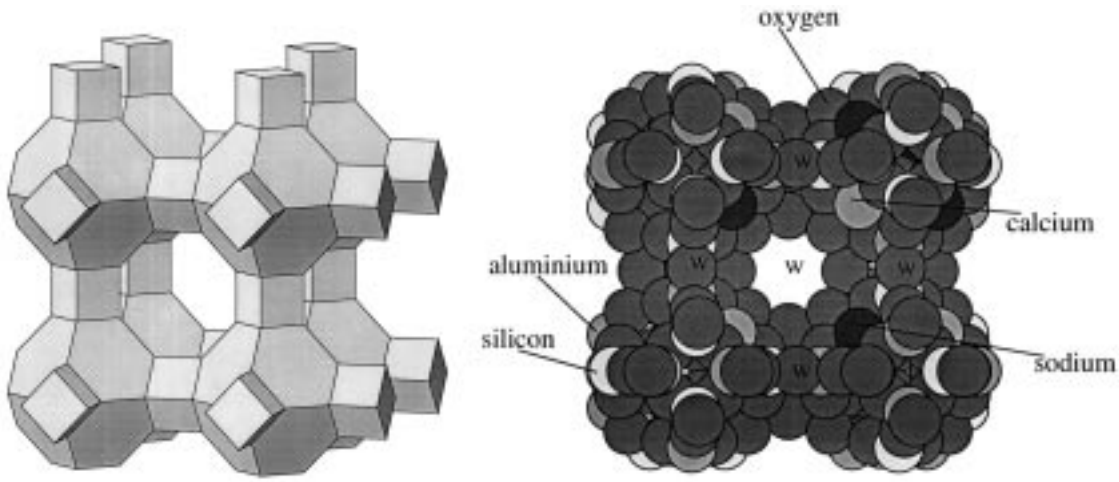

Fig. 1. Structure of zeolites of type LTA (left: general sight; right: internal view).

2. Statistical and numerical background

Statistical physics built a bridge between the macroscopic properties of the systems considered and the microscopic properties of the particles included in the systems [4–7].

2.1. Statistical quantities and relations

Equilibrium properties can be evaluated using the statistical quantities *partition function*, or, in the case of computer simulations, more appropriate *radial distribution functions*, while transport coefficients can be calculated using *correlation functions*. Here we will give the relations necessary to determine diffusion coefficients only.

2.1.1. Correlation functions

Using the *ensemble average* in the Γ-space

$$\langle A\rangle_\Gamma = \int\int A(q(t),p(t))\rho^{(N)}(q(t),p(t))\mathrm{d}q\mathrm{d}p \tag{1}$$

with the *equilibrium* phase space density $\rho^{(N)}(q(t),p(t))$ the classical *time correlation functions*

$$K_{AB}(t) = \langle A(t)B(0)\rangle_\Gamma$$

$$= \int\ldots\int A(q,p,t)B(q,p,0)\rho^{(N)}(q,p)\mathrm{d}q\mathrm{d}p \tag{2}$$

for the phase space functions $A\{q(t),\ p(t)\} = A(t)$ and $B\{q(t),\ p(t)\} = B(t)$ are defined by Eq. (2). With $A = B$, $K_{AA}(t)$ is called *auto correlation function*; for $A = B = \vec{v}$ (velocity): *velocity auto correlation function* $K_{vv}(t)$.

The *linear response* theory of Kubo [32,33] relates transport coefficients to the corresponding auto correlation functions using Fourier transformations.

Here we need only the relation for the (self-) diffusion coefficient, given in the long-wave limit $\omega \to 0$, $k \to 0$,

$$D = \frac{1}{3}\int_0^\infty \langle \vec{v}(t)\cdot\vec{v}(0)\rangle \mathrm{d}t \tag{3}$$

Equivalent to Eq. (3) the diffusion coefficient can be calculated either by the mean square displacements which are available from MD simulations and pulsed field gradient nuclear magnetic resonance measurements (PFG-NMR) as well [3,6]

$$2t\mathrm{D} = \frac{1}{3}\lim_{t\to\infty}\langle(\vec{r}(t)-\vec{r}(0))^2\rangle \tag{4}$$

or using the decay of the self-part $F_s(k,t)$ of the *intermediate scattering function* (see Eq. (18) below).

2.1.2. Propagators

The so-called propagator gives additional insights into microscopic details of diffusion processes. It serves moreover, together with the scattering function, as an additional possibility in determining diffusion coefficients.

The *propagator* is defined as the conditional probability density to find a particle at time t at the place $\vec{r}$ if it has been

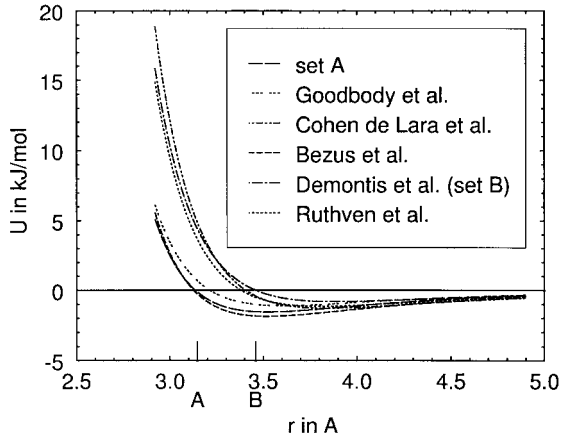

Fig. 2. LJ potentials (CH_4-O interaction from literature [10–14,36–45]).

at time $t = 0$ at $\vec{r}_0$. For a pure random walk the propagator is a Gaussian distribution

$$P(\vec{r},t) = (4\pi Dt)^{-\frac{3}{2}} \exp\left\{-\frac{(\vec{r}-\vec{r}_0)^2}{4Dt}\right\} \quad (5)$$

For the validity of the diffusion equation, it is necessary and sufficient that all moments $\langle f(\vec{r})^\nu \rangle$ of $f(\vec{r}) = (\vec{r}-\vec{r}_0)$ (Eqs. (5) and (6)) will give the same diffusion coefficient. Using the first four moments ($\nu = 1, 2, 3, 4$) it was shown that the diffusion equation is valid even for few particles in narrow pores after a certain time [35]. Applying the definition

$$\langle f(\vec{r})^\nu \rangle = \int P(\vec{r},t) f(\vec{r})^\nu d\vec{r} \quad (6)$$

we find for the second moment ($\nu = 2$) of this distribution again Eq. (4)

$$\langle (\vec{r}-\vec{r}_0)^2 \rangle = 6Dt \quad (7)$$

2.2. Intermolecular potentials

In comparing simulation results with experimental data the intermolecular potentials used in the simulations are of fundamental importance. Here we choose Lennard-Jones [12,6] potentials)

$$U = 4\epsilon\left\{\left(\frac{\sigma}{r}\right)^{12} - \left(\frac{\sigma}{r}\right)^{6}\right\} \quad (8)$$

with ϵ denoting the minimum value of the potential energy and σ defined by $U(\sigma) = 0$ for the short-range interaction [7]. Often this one and other empirical potential functions are used, because quantum-chemical calculations of potential surfaces are restricted to not too complex systems although they made large progress [34].

In the case of the NaCaA zeolite where exchangeable cations Na^+ and Ca^{2+} are taken into account (see Fig. 3) another term for the polarization energy U_p is added for each guest molecule

$$U_p(\vec{r}) = -\frac{\alpha}{2}\vec{E}(\vec{r})^2 \quad (9)$$

α is the polarizability of the guest molecule and $\vec{E}(\vec{r})$ the electric field at the site $\vec{r}$. This term gives the interaction energy of the induced dipole with the electric field while the dipole-dipole interaction of the induced dipoles of different guest molecules is considered to be a second order correction as well as back-polarization effect. The aim of this investigation was to show the strong influence of the induction energy on diffusion of a small neutral molecule in a zeolite. Higher accuracy could not be expected since the simple model proposed by Ruthven and Derrah [36] was used to get effective cation diameters. Hence higher order terms have been neglected. It is worthwhile to notice that even this simple treatment involves three body interactions because $\vec{E}$ is a sum of contributions from different cations and lattice oxygens so that the square contains mixed terms. For the charge distribution in the lattice the model proposed in [36] is used that asigns a charge of $-0.25e$ to each oxygen and treats the other lattice atoms as uncharged.

The potential data for the diffusion of CH_4/Xe mixtures in silicalite are taken from [14] for methane (to have a comparison for pure methane with the literature data) and from [15] for xenon. For the interaction of xenon with methane they are calculated using the rule of Lorentz-Berthelot [7].

Fig. 2 (right) shows the contributions of the different interactions.

In Fig. 2 LJ potentials with different potential parameters used in the literature for the methane-oxygen interaction in LTA-zeolites [10–14,36–45] are given (labels A, B for the σ-values at the abscissa), given in Table 1. Test calculations showed that the interaction of the guest molecules with the other lattice atoms can be neglected. In order to check the importance of the variation particularly of the σ-parameter in the literature we introduced parameter sets A and B which are representative for the two groups of potentials to be seen in Fig. 2 (here there is no difference between the potential of Demontis et al. [12,37–41] and set B to be seen). Even more important was the goal to examine whether and how the diffusion mechanism is influenced by details of the pore geometry (Fig. 3).

Figs. 4 and 5 compare the used potential sets A and B for methane guest molecules in ZK4. It is to be seen that for set A a potential minimum is practically in the window (Fig. 5, left), while for set B the minimum is in front of the windows (Fig. 5, right), which means that the diffusing particle must get over a potential barrier to migrate to the next large cavity.

3. Results

3.1. Propagators

The form of the propagators (Eq. (5)) give some hints about the diffusion. Fig. 6 (left) gives the ideal Gaussian form (see Eq. (5)), while for the migration of methane guest

Table 1

Parameter sets used for the LJ potential (Eq. (8))

Zeolite		σ (Å)	ϵ (kJ/mol)
LTA	CH_4–CH_4	3.817	1.232
LTA	CH_4–Si	2.14	0.29
LTA	CH_4–O (set A)	3.14	1.5
LTA	CH_4–O (set B)	3.46	0.81
LTA	C_2H_6–O	3.775	1.536
Silicalite	CH_4-CH4	3.730	1.230
Silicalite	CH_4–O	3.214	1.108
Silicalite	CH_4–Xe	3.897	1.517
Silicalite	Xe–Xc	4.064	1.870
Silicalite	Xe–O	3.296	1.679

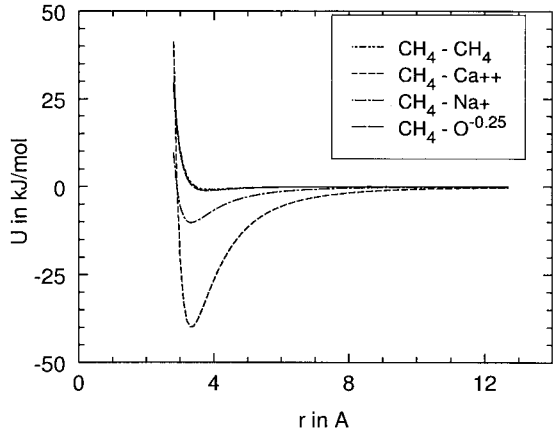

Fig. 3. LJ potentials for different isolated pairs.

molecules through ZK4 characteristic changes arise due to the structure of the zeolite (light).

Fig. 7 describes the time development of the propagator $P(x,y,t)$ of ethane in ZK4 and shows a structural behaviour equivalent to that for methane in Fig. 6 (right).

Up to now the experimental determination is restricted due to the limited resolution of the PFG NMR experiments which is shown in Fig. 8. The calculated values may serve as challenge for the experimentalists to improve their methods using, e.g. neutron scattering.

More general relations can be derived connecting the propagator with the self-part of van Hove's correlation function [24,25]. We denote (in the one-dimensional case) by $P(x, t)$ the probability density of finding a particle near the position x at time t, by $P(x_1, t_1; x_0,t_0)$ the probability density of finding a particle near x_0 at time t_0 and near x_1 at time t_1, and by $p(x_1, t_1|x_0, t_0)$ the corresponding *transition probability*, also known as the *propagator* of $P(x,t)$ due to the relation

$$P(x_1, t_1) = \int p(x_1, t_1|x_0, t_0)P(x_0, t_0)\mathrm{d}x_0 \tag{10}$$

The self-part of the van Hove function, $G_s(x,t)$, is defined as the probability that a particle moves within the time t by the distance x. For instance the mean value of $P(x_1,t_1; x_0,t_0)$ over all initial positions x_0 under the constraints $x_1 - x_0 = x$ and $t_1 - t_0 = t$ is given by

$$G_s(x, t) = \lim_{L\to\infty} \frac{1}{2L}\int_{-L}^{L} P(x_0 + x, t_0 + t; x_0, t_0)\mathrm{d}x_0 \tag{11}$$

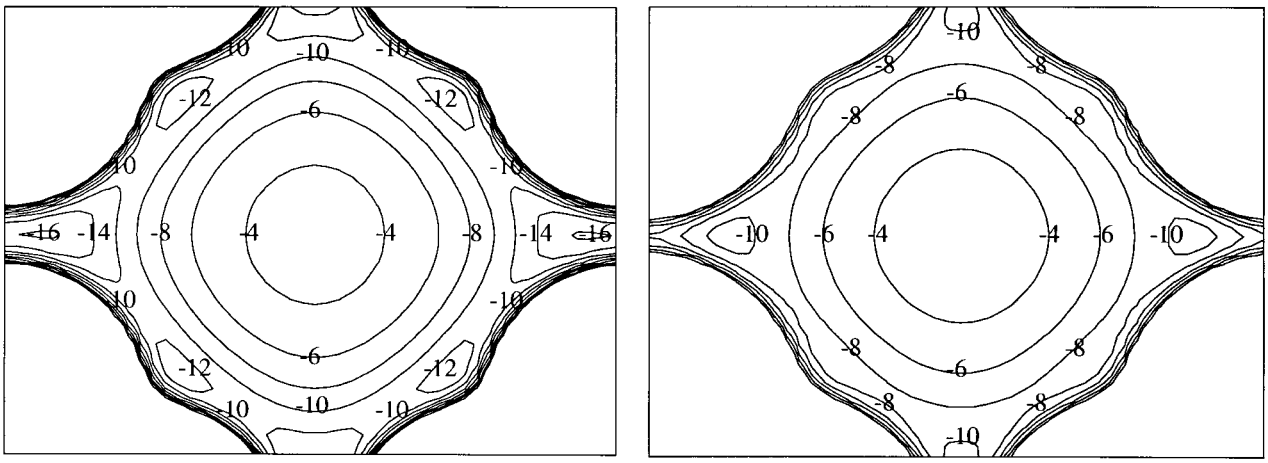

Fig. 4. Potential surface (left: set A; right: set B) cut through the center and four windows of the cavity (U in kJ/mol).

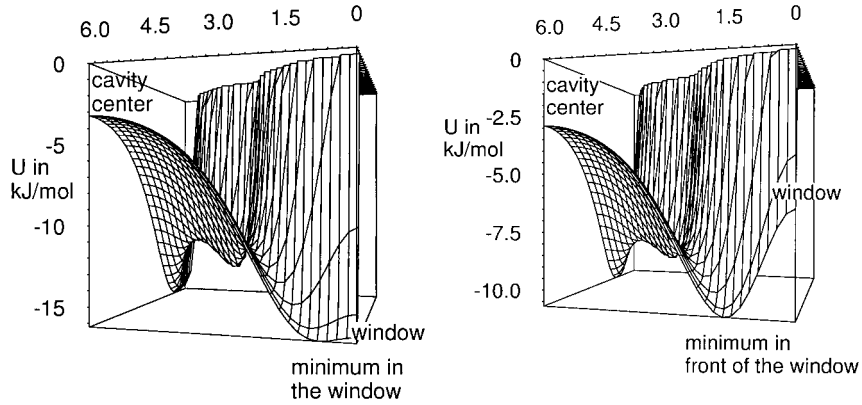

Fig. 5. Potential surface (left: set A; right: set B).

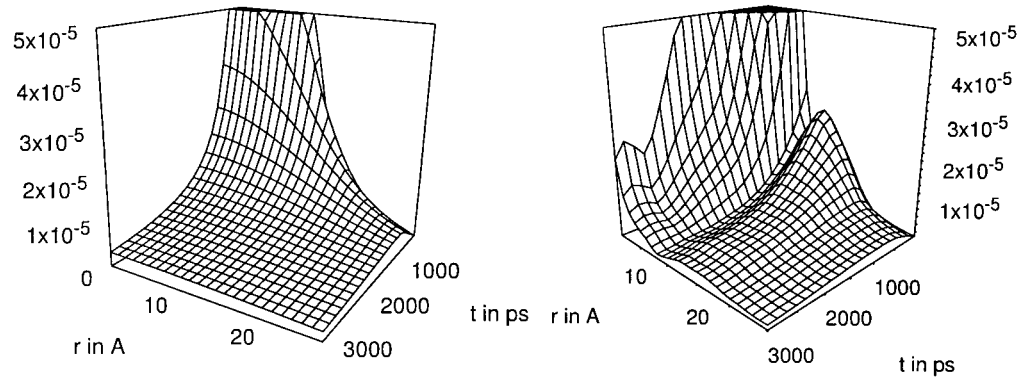

Fig. 6. Propagator $P(\vec{r}, t)$ as a function of $\vec{r}$ and t (set B, I = 3, T = 300 K) in ideal bulk systems (left) and ZK4 (right).

Using the relation

$$P(x_1, t_1; x_0, t_0) = p(x_1, t_1 | x_0, t_0) P(x_0, t_0) \tag{12}$$

we find

$$G_s(x,t) = \lim_{L\to\infty} \frac{1}{2L} \int_{-L}^{L} p(x_0 + x, t_0 + t | x_0, t_0) P(x_0, t_0) \mathrm{d}x_0 \tag{13}$$

In the case of a homogeneous medium (e.g. a liquid) in a stationary state, P and p become independent of x_0 and t_0 yielding

$$G_s(x,t) = p(x,t|0,0) \tag{14}$$

If the diffusion equation holds one gets

$$p(x,t|0,0) = \frac{1}{\sqrt{4\pi D t}} \exp\left[-\frac{x^2}{4Dt}\right] \tag{15}$$

For a crystal of period a, under special conditions regarding the time scales of motion, $G_s(x,t)$ may be approximated by

$$G_s(x,t) = p(x,t|0,0) \frac{1}{a} \int_0^a P(x_0 + x) P(x_0) \mathrm{d}x_0 \tag{16}$$

A detailed discussion of G_s for intra-zeolite diffusion can be found in [24,25] (Figs. 9 and 10. Its spatial Fourier transform yields the self-part F_s(k,t) of the *intermediate scattering function*. For fluids or in the hydrodynamic limit, F_s decays exponentially

$$F_s(\boldsymbol{k}, \boldsymbol{t}) \sim \exp(-\boldsymbol{k^2 D t}) \tag{17}$$

Consequently, in that time region is valid:

$$D = \frac{\ln F_s(\boldsymbol{k}, \boldsymbol{0}) - \ln \boldsymbol{F}_s(\boldsymbol{k}, \boldsymbol{t})}{k^2 t} \tag{18}$$

In Table 2 self-diffusion coefficients for methane guest molecules calculated in this manner are given for T = 300 K.

3.2. Density distributions

The density distributions of methane in a cation-free LTA in Fig. 11 demonstrated in a plane through the center of the large cavity, show a remarkable structure too. Corresponding to the potential surface these distributions are different from zero practically only near the cavity wall and these densities have maxima in the window (left: set A) and *in front of* them (right: set B), respectively.

The density distribution of methane in the cation-free LTA zeolite may well be understood by the potentials (see Figs. 4 and 5) and [47]. These different density profiles will yield different diffusion behaviour for both cases of course (see Figs. 13, and 15). A similar situation was found for ethane in ZK4 (see Fig. 12).

3.3. Diffusion coefficients

3.3.1. Methane in LTA-zeolites

Fig. 13 (left) shows that the diffusion coefficient D increases with increasing mean number of guest molecules per cavity and temperature for set B (smaller window) while this dependence for set A (larger window), demonstrated for T = 173°K, is reversed (right)[1]. This is understandable taking into account the probability, and its different dependence on loading and window size, for a guest molecule, firstly to find the way through the window and secondly to be pushed back by other guest molecules. These effects result in increasing diffusion with increasing loadings in the case of smaller windows (set B). Such behaviour, in contrast to the well-known density dependence of diffusion coefficients in bulk fluids, which is still under examination, was found experimentally by pulsed field gradient (PFG) NMR experiments and compared with other patterns of concentration dependencies and can be explained by the different spatial conditions for different guest molecules in different zeolites [3] (Fig. 14).

For higher loading this figure shows an interesting cross over of both curvatures which is under examination in detail. Increasing diffusivity with increasing concentration is in fact the behaviour found for paraffin in A type zeolites experimentally by PFG-NMR [3].

[1] Additional calculations with the same ϵ-values have shown that for diffusion coefficients for zeolites with such small window changes in D caused by variations of ϵ are small compared with those caused by σ-variations [21]. This is obviously not valid for adsorption.

For extreme high loadings the diffusion will be restricted by the steric hindrance of the large number of the guest molecules in the narrow pores (R. Haberlandt, S. Fritzsche, 1992, unpublished data) [49] (see Fig. 17 (right) for ethane molecules in ZK4).

3.3.2. Influence of lattice vibrations on the diffusion coefficients

In contrary to the initial results of Demontis and Suffritti [49] the influence of lattice vibrations on the diffusion coefficient in the cation-free LTA zeolite is not very large for both of the parameter sets under consideration [20,21] which is shown in Fig. 15 for different σ (left) and different temperatures (right).

3.3.3. Influence of cations on D

The dynamics even of small neutral molecules with saturated bindings is strongly influenced by the presence of exchangeable cations [50,52]. This is investigated for the NaCaA zeolite with 4 Na^+ and 4 Ca^{2+} ions. In this case the windows, marked by *w* in Fig. 1 (right), are free from cations. The unexpected [52] strong effect can clearly be seen in Fig. 16 (left) and has been confirmed experimentally, meanwhile [53]. In comparison with the cation-free LTA the self-diffusivity decreases up to two orders of magnitude. It should be noted that the computational effort is much larger in this case than in the simulations for the cation-free form since much longer trajectories (up to 5–10 ns) are necessary to evaluate such small diffusivities.

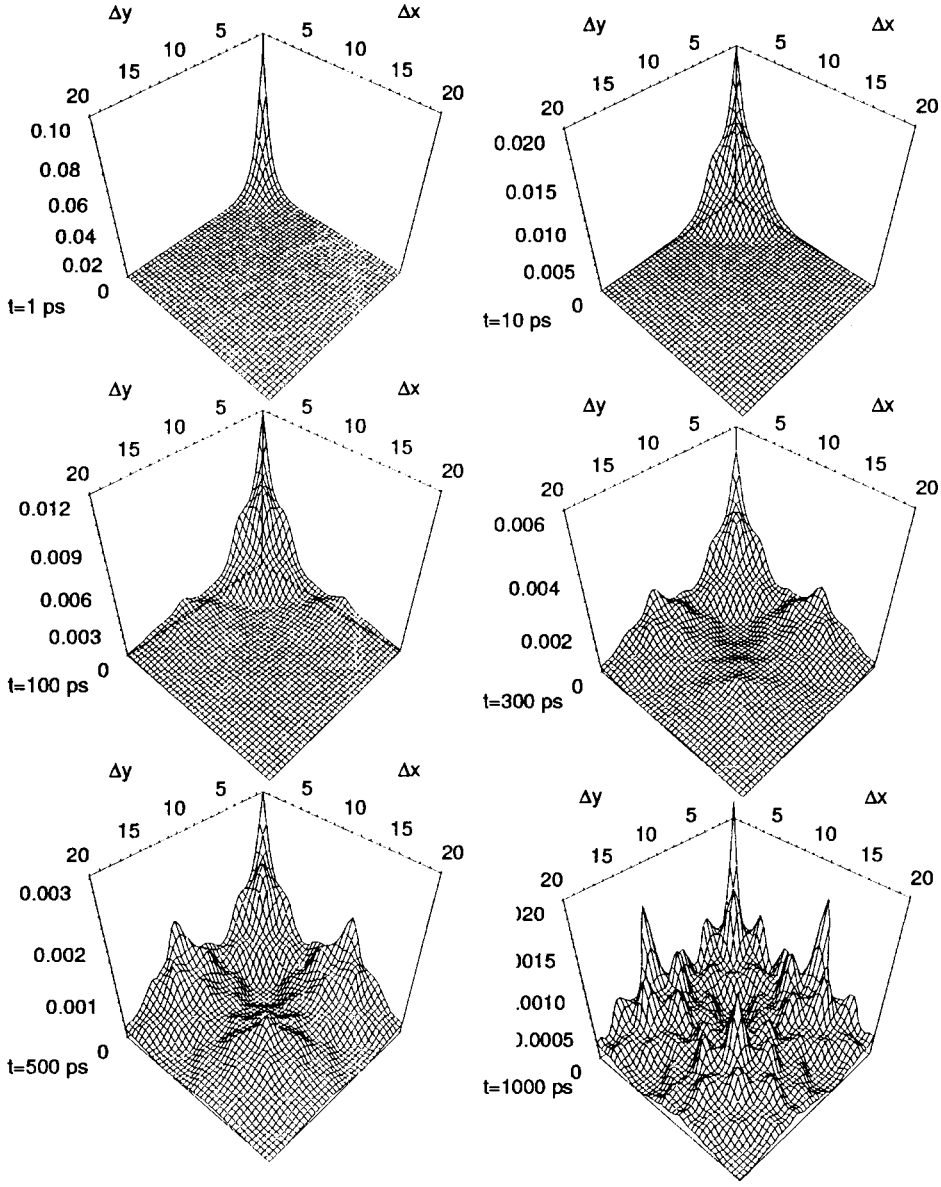

Fig. 7. Two dimensional graph of the time development of the propagator $P(x,y,t)$ – Δx, Δy in Å; t in ps – calculated from a trajectory (set A, I = 3, T = 300 K).

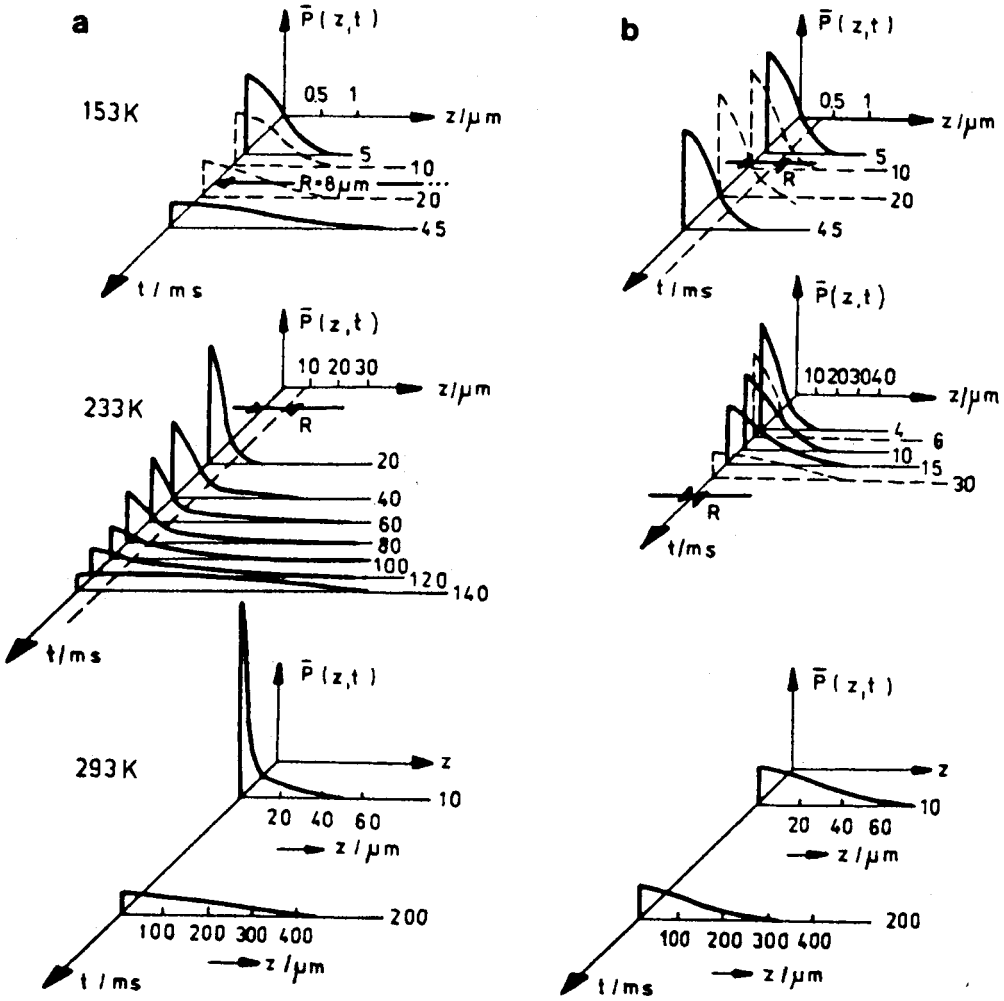

Fig. 8. Propagator representation of the self-diffusion of ethane in NaCaA zeolite for two different size fractions r_c of the crystals: (a) 40 mg/g, r_c = 8 μm; (b) 58 mg/g, r_c = 0.4 μm (with permission from [3]).

Additionally, the calculation of the forces resulting from the polarization energy is very time-consuming although the full Ewald sum can be replaced by a corrected *r* space part of this sum [21]. Fig. 16 (left) demonstrates MD results for the NaCaA zeolite and its cation-free analogue which has the same structure and compares these data with experimental results from PFG-NMR measurements [19] of methane diffusion in the NaCaA zeolite. The comparison shows that the simulation results for *D* are strongly influenced by the presence or lack of cations. They furthermore show that the calculations that employ set A and take into account the polarization interaction fit the experimental results better than the other interactions used in this examination. The agreement is good at high loadings but it is less satisfactory at low loadings. Meanwhile, experimental in-vestigations which where initiated by our first results have confirmed this strong influence of the polarization interaction on the diffusion even of neutral molecules which have no unsaturated bindings [53].

3.3.4. Transport-diffusivity, corrected diffusivity and self-diffusivity

While the self-diffusion coefficient *D* according to the Kubo theory may be obtained from [4,6,33,54] (Eq. (19))

$$D = \frac{1}{3}\sum_J \int_0^\infty \mathrm{d}t\, \langle \vec{v}_j(0)\vec{v}_j(t)\rangle \tag{19}$$

the so-called corrected diffusion coefficient D_c includes the cross-correlations between velocities of different particles

$$D_c = \frac{1}{3}\sum_j \sum_K \int_0^\infty \mathrm{d}t\, \langle \vec{v}_j(0)\vec{v}_k(t)\rangle \tag{20}$$

The diffusion coefficient that appears in Fick's law is often called transport diffusion coefficient D_T [3],which is not only from a scientific but from a practical interest too [46]

$$J = -D_T \frac{\mathrm{d}n}{\mathrm{d}x} \tag{21}$$

J is the flux and *n* is the density connected with the stream velocity *v* by $J = nv$. If the force *F* in the well-known

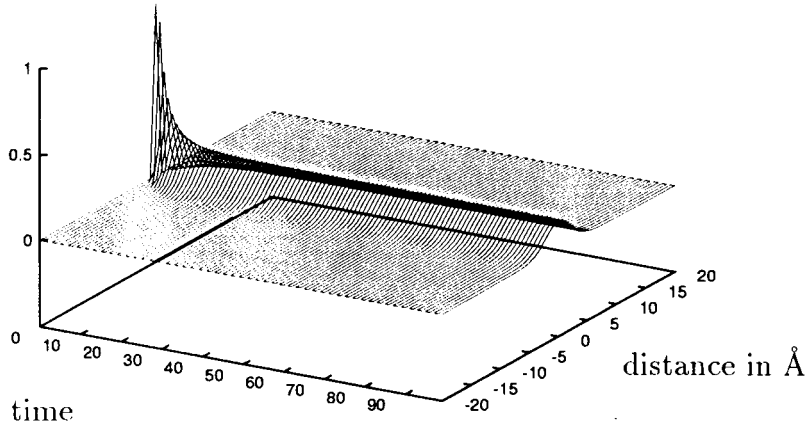

Fig. 9. $G_s(x,t)$ for a liquid (arbitrary units).

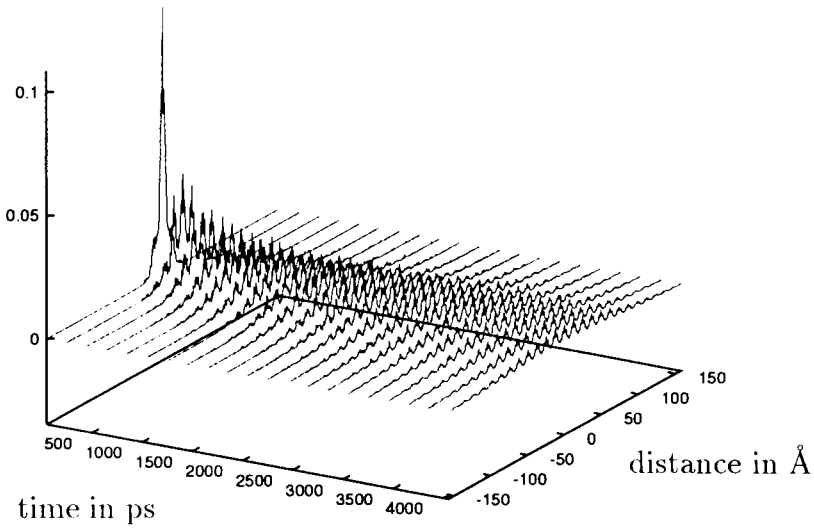

Fig. 10. $G_s(x,t)$ for methane CH_4 in ZK4.

relation (Eq. (22))

$$v = BF \tag{22}$$

is substituted by gradient of the chemical potential μ one has

$$J = -nB\frac{d\mu}{dx} \tag{23}$$

where B is the mobility. According to Kubo's theory B is connected with the corrected diffusivity by the relation

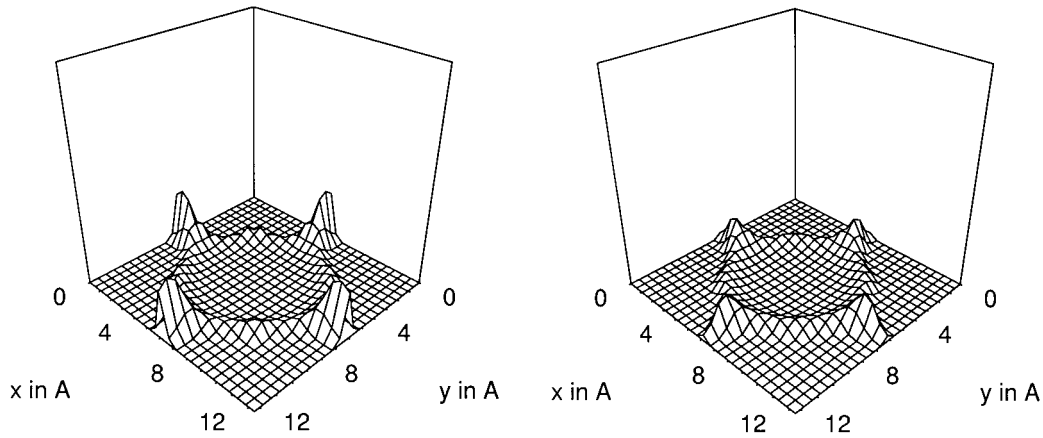

Fig. 11. Density distribution (in arbitrary units) of methane in a cation-free LTA (left: set A; right: set B).

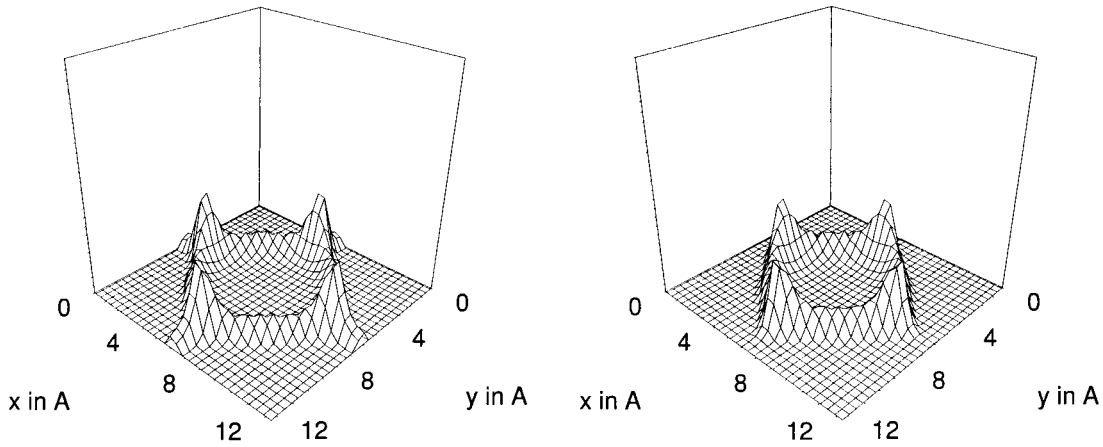

Fig. 12. Density distribution (in arbitrary units) of ethane in a cation-free LTA (left: set A, right: set B).

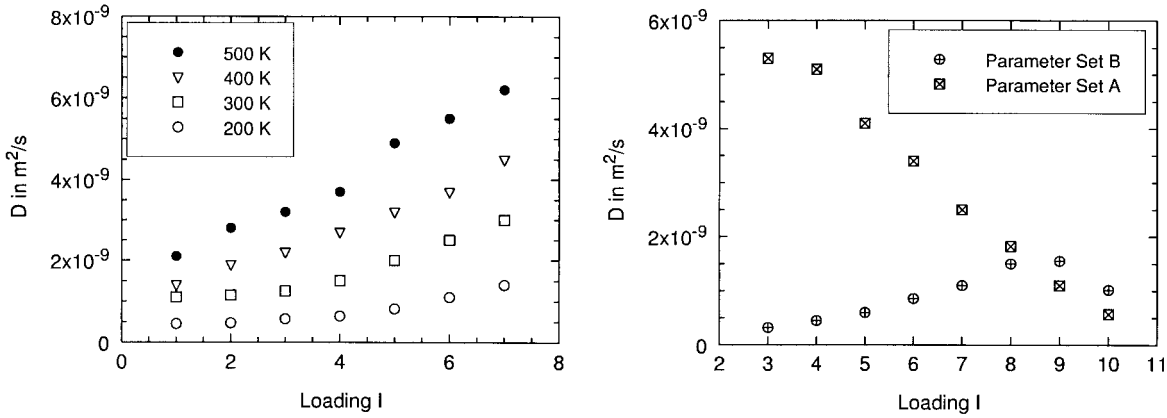

Fig. 13. Diffusion coefficient D for different loadings of methane in the cation-free LTA zeolite (left: different temperatures T, set B; right: T = 173°K, set A, B).

$$D_c = Bk_BT \tag{24}$$

where k_B is the Boltzmann constant. Comparison of Eqs. (21) – (24) leads to (Eq. (25))

$$D_T = D_c \frac{n}{k_BT}\frac{d\mu}{dn} \tag{25}$$

which is a form of the well-known Darken equation [3]. In Fig. 16 (right) these different diffusivities obtained from equilibrium and non-equilibrium MD simulations are compared with each other. The self-diffusion coefficients have been obtained from the mean square displacement. D_T results from non-equilibrium simulations in which a density gradient in six layers of cavities is created by ran-

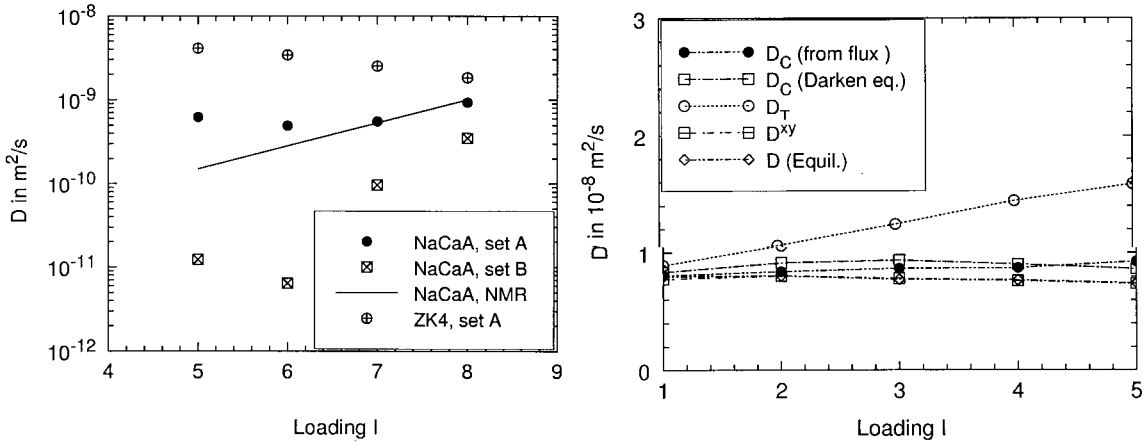

Fig. 16. Different diffusion coefficients: left, comparison of D of methane in NaCaA and cation-free LTA with NMR-experiments; right, self-diffusion coefficient D, corrected diffusion coefficient D_c and transport-diffusion coefficient D_T from non-equilibrium MD.

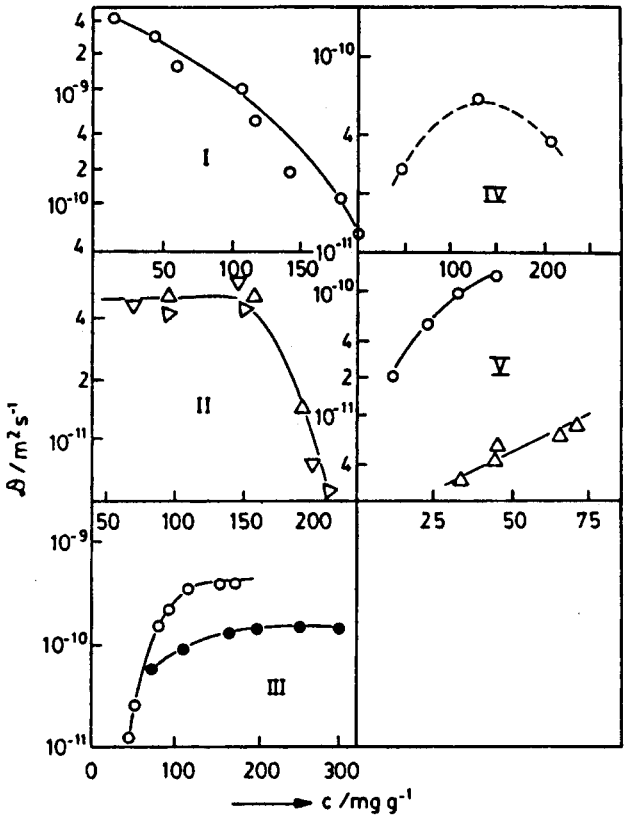

Fig. 14. Patterns of concentration dependence of self-diffusivities (I: *n*-hexane in NaX at 358 K; II: ortho (△), meta (▷) and para (▽) xylenes in NaX at 393 K; III ammonia (○) and water (●) in NaX at 298 K; IV: acetonitrile in NaX at:393 K; V: ethane (○) at 173 K and propane (▽) at 413 K in NaCaA - with permission from [3]).

domly inserting particles that leave the last layer into the first layer and evaluating the flux in the intermediate region [54]. D^{xy}, obtained from the mean square displacement perpendicular to the density gradient, is equal of course to the self-diffusion coefficient D (Equil.). It turns out that the flux practically has no influence the self-diffusion in the direction perpendicular to the flux. D_c is somewhat larger than D which might be attributed to the collective

Table 2

D in ZK4 from the decay of the first components of the scattering function (time recorded: t = 4095 ps)

n_{occ}	k	F_s (k,t)	D (10^{-9} m^2/s)
3	Δk	0.430	8.17 (9.46)
6	Δk	0.508	7.14 (7.19)
9	Δk	0.865	3.87 (3.56)
	$2\Delta k$	0.074	4.75
12	Δk	1.295	1.39 (1.42)
	$2\Delta k$	0.696	1.30
	$3\Delta k$	0.282	1.20
15	Δk	1.505	0.12 (0.12)
	$2\Delta k$	1.216	0.11
	$3\Delta k$	0.896	0.10

Values from mean square displacement are shown in parentheses.

effects expressed by the cross-correlation terms in Eq. (20). D_c is obtained from D_T by the Darken equation and compared with results from another non-equilibrium MD experiment. In this experiment a flux is produced by an external force field. Measuring this flux D_c may be obtained from Eq. (24). Equivalent results are derived using the Kubo theory [24].

3.3.5. Ethane in ZK4

The evaluated diffusion coefficients of ethane (set B) increase with increasing loading (Fig. 17, left) as those for methane (compare Fig. 13, left). Both show Arrhenius behavior [30,47]. For extreme high loadings diffusion coefficients of ethane will strongly decrease (Fig. 17, right)).

Of course for very high loadings the diffusion coefficients diminish rapidly due to the steric conditions [49], as demonstrated here by Fig. 17 (right) for ethane guest molecules in ZK4.

3.3.6. CH_4/Xe in silicalites

The diffusion of binary mixture of methane and xenon in silicalite was examined using MD-simulations and PFG-

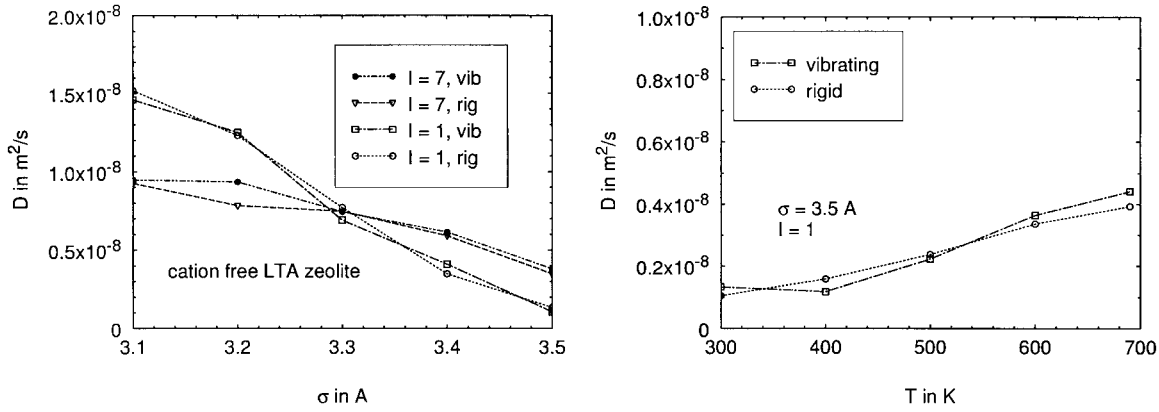

Fig. 15. Comparison of D with rigid and vibrating lattice in dependences on σ for two loadings (left) and in dependence on the temperature (right).

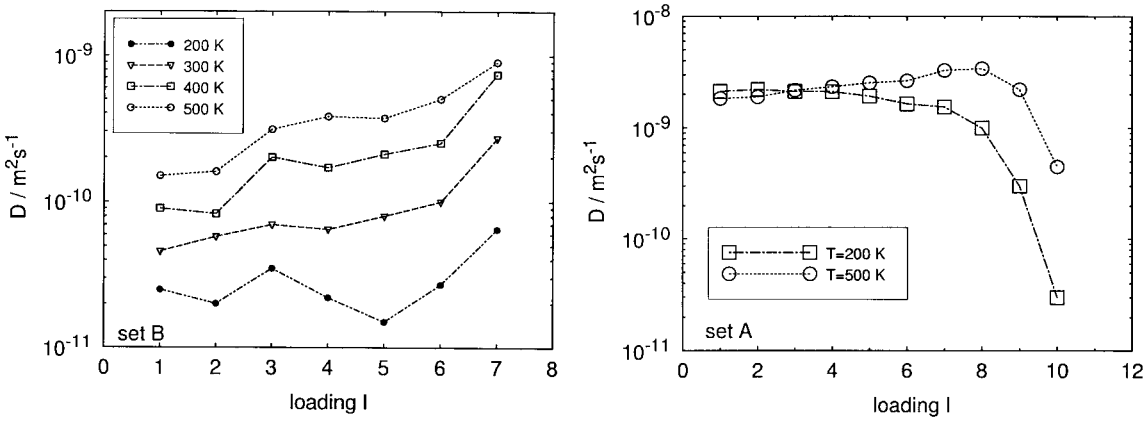

Fig. 17. Diffusion of ethane in ZK4 in dependence on the loading I for different temperatures T (left: set B, right: extreme high loadings).

NMR experiments [28]. Of special interest are the changes in diffusive behaviour in the presence of the other diffusing species.

Fig. 18 allows the calculated diffusion coefficients for different quotas of xenon and methane in good accordance with the experimental values. The total loading of guest molecules is held constant (eight guest molecules per unit cells, but the ratio of methane to xenon is varied from pure methane (at the left of each figure) to pure xenon (at the right). In the case of one pure species in the zeolite the diffusion coefficient of methane is about six times larger than the one of xenon (simulation). With increasing xenon quota the methane diffusion is slowed down until the diffusion coefficient reaches nearly the value of xenon for high xenon quotas. For the same range of different parameters there is nearly no change in the diffusion coefficients of xenon, so we have an obviously asymmetric behaviour in the mixture. That means, the xenon diffusion dominates the diffusion of methane.

One reason for this strong influence of the xenon on the methane lies in the topology of the silicalite. The channels within the silicalite have a slightly eliptical cross section with a diameter of about 5.3 Å. In these narrow tubes there are no possibilities for the faster methane molecules to pass the slower xenon atoms. Only in the cross sections overtaking might be possible. Therefore at high xenon loadings the methane molecules can rattle within a cage of xenon neighbours only.

4. Conclusions

Statistical physics and molecular dynamics provide a good basis for the detailed understanding of the diffusion processes in porous media. This was demonstrated by the evaluation of diffusion coefficients of guest molecules in zeolites and the good agreement with experimental data. These results are a valuable basis to investigate more complex processes in zeolites, as e.g. chemical reactions influenced by catalysts.

Acknowledgements

I am greatly indebted to my coworkers Dr. S. Fritzsche, DP M. Gaub, DP G. Hofmann, DP S. Jost, DP A. Schüring

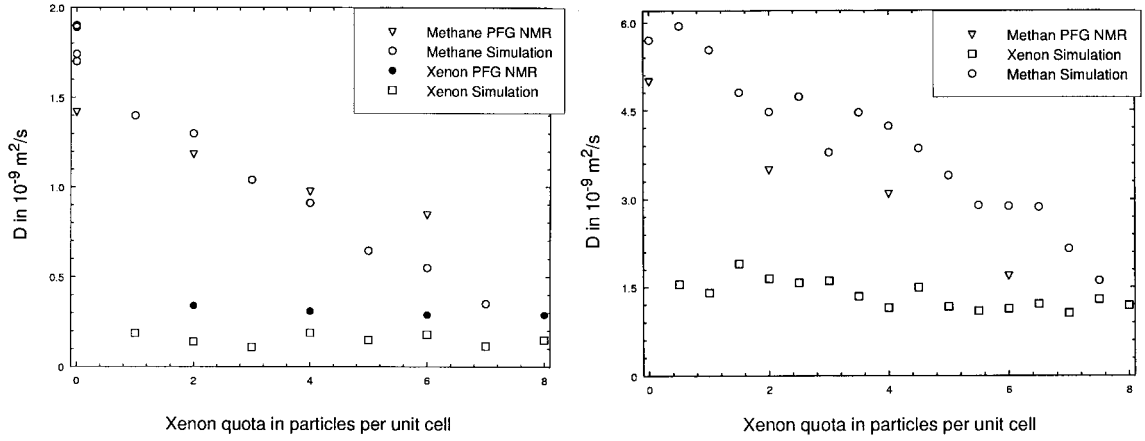

Fig. 18. The three dimensional diffusion coefficient for a total loading of eight guest molecules per unit cell at temperatures (left) $T = 152$ K and (right) $T = 29.3$ K.

and to Prof. J. Kärger (Leipzig), M. Wolfsberg (UCI) for their valuable contributions to the results presented here. Moreover I thank Professors H. Pfeifer (Leipzig), G. Suffritti, G. Demontis (University of Sassari), D. Theodorou (University of Patras), M. Schoen (Wuppertal/Berlin) and Dr. K. Heinzinger (MPI for Chemie, Mainz) for a lot of stimulating discussions and the referees for valuable hints. This research is supported by the Deutsche Forschungsgenmeinschaft (SFB 294) and the Fonds der Chemischen Industrie, Frankfurt.

References

[1] D.W. Breck, Zeolite Molecular Sieves, Wiley, New York, 1974.
[2] W.M. Meier, D.H. Olson, Atlas of Zeolite Structure Types, Butterworth–Heinemann, London, 1992.
[3] J. Kärger, D.M. Ruthven, Diffusion in Zeolites and Other Microporous Solids, Wiley, New York, 1992.
[4] D.A. McQuarrie, Statistical Mechanics, Harper and Row, New York, 1976.
[5] M.P. Allen, T.S. Tildesley, Computer Simulation of Liquids, Clarendon Press, Oxford, 1989.
[6] R. Haberlandt, S. Fritzsche, G. Peinel, K. Heinzinger, Molekulardynarnik, Vieweg, Wiesbaden, 1995.
[7] J.O. Hirschfelder, C.F. Curtiss, R.B. Bird, Molecular Theory of Gases and Liquids, Wiley, New York, 1954.
[8] P. Demontis, G.B. Suffritti, Structure and Dynamics of Zeolites Investigated by Molecular Dynamics, Chemical Reviews, 97 (1997) 2845.
[9] S. Yashonath, P. Demontis, M. Klein, Chem. Phys. Lett. 153 (1988) 551.
[10] E. Cohen de Lara, R. Kahn, A.M. Goulay, J. Chem. Phys. 90 (1989) 7482.
[11] S. Fritzsche, R. Haberlandt, J. Kärger, H. Pfeifer, M. Wolfsberg, Chem. Phys. Lett. 171 (1990) 109.
[12] P. Demontis, G.B. Suffritti, E.S. Fois, S. Quartieri, J. Phys. Chem. 94 (1990) 4329.
[13] P.L. June, A.T. Bell, D.N. Theodorou, J. Phys. Chem. 94 (1990) 8232.
[14] S.J. Goodbody, K. Watanabe, D. MacCowan, J.P.R.B. Walton, N. Quirke, J. Chem. Faraday Trans. 87 (1991) 1951.
[15] S. Pickett, A. Nowak, J. Thomas, et al., J. Phys. Chem. 94 (1990) 1233.
[16] C.R.A. Catlow, C.M. Freeman, B. Vessal, S.M. Tomlinson, M. Leslie, J. Chem. Faraday Trans. 87 (1991) 1947.
[17] G. Schrimpf, M. Schlenkrich, J. Brickmann, P. Bopp, J. Phys. Chem. 96 (1992) 7404.
[18] D.N. Theodorou, R.Q. Snurr, A.T. Bell, Molecular Dynamics and Diffusion in Microporous Materials, in C.T. Alberti, T. Bein (eds.), Comprehensive Supramolecular Chemistry, Vol. 7, Pergamon, Oxford, 1996, p. 507.
[19] W. Heink, J. Kärger, H. Pfeifer, P. Salverda, K.P. Datema, A. Nowak, J. Chem. Soc. Faraday Trans. 88 (1992) 515.
[20] S. Fritzsche, M. Gaub, R. Haberlandt, C. Hofmann, J. Mol. Model. 2 (1996) 286.
[21] S. Fritzsche, Habilitationsschrift, University Leipzig, 1998 (submitted).
[22] S. Fritzsche, M. Wolfsberg, R. Haberlandt, P. Demontis, G.B. Suffritti, Influence of Lattice Vibrations on Diffusion in LTA Zeolites (in press).
[23] G. Hofmann, Dissertation, University Leipzig, 1998.
[24] M. Gaub, Dissertation, University Leipzig, 1998 (submitted).
[25] M. Gaub, S. Fritzsche, R. Haberlandt, D. Theodorou, Diffusion in Zeolites Using the Van Hove Function (in press).
[26] S. Jost, Diploma thesis, University Leipzig, 1997.
[27] S. Jost, S. Fritzsche, R. Haberlandt, Chem. Phys. Lett. 279 (1997) 385.
[28] S. Jost, N.K. Bär, S. Fritzsche, R. Haberlandt, J. Kärger, The diffusion of a mixture of methane and xenon in silicalite: an MD-study and PFG-NMR experiments (in press).
[29] A. Schüring, Diploma thesis, University Leipzig, 1997.
[30] A. Schüring, S. Fritzsche, R. Haberlandt (in press).
[31] S. Fritzsche, R. Haberlandt, G. Hofmann, J. Kärger, K. Heinzinger, M. Wolfsberg, Chem. Phys. Lett. 265 (1997) 253.
[32] R. Kubo, J. Phys. Soc. Japan 12 (1957) 570.
[33] R. Kubo, M. Toda, N. Hashitsume, Statistical Physics. II. Nonequilibrium Statistical Mechanics, Springer, Berlin, 1991.
[34] J. Sauer, P. Ugliengo, E. Garrone, V.R. Saunders, Chem. Rev. 94 (1994) 2095.
[35] S. Fritzsche, R. Haberlandt, J. Kärger, H. Pfeifer, K. Heinzinger, Chem. Phys. Lett. 198 (1992) 283.
[36] D.M. Ruthven, R.I. Derrah, J. Chem. Soc. Faraday Trans. 68 (1972) 2332.
[37] P. Demontis, G.B. Suffritti, E.S. Fois, S. Quartieri, J. Phys. Chem. 96 (1992) 1482.
[38] P. Demontis, G.B. Suffritti, P. Mura, Chem. Phys. Lett. 191 (1992) 553.
[39] P. Demontis, G.B. Suffritti, Molecular Dynamics Studies in Zeolites, in C.R.A. Catlow (ed.), Modelling of Structure and Reactivity in Zeolites, Herausgeber, Academic Press, London, 1992, p. 79.
[40] P. Denwontis, G.B. Suffritti, Chem. Phys. Lett. 223 (1994) 355.
[41] P. Demontis, G.B. Suffritti, Molecular dynamics simulations of diffusion in a cubic symmetry zeolite, in J. Weitkamp, H.G. Karge, H. Pfeifer, W. Hoelderich (eds.), Proc. 10th Int. Zeolite Conf., Elsevier, Amsterdam, 1994, p. 2107.
[42] A.G. Bezus, A.V. Kiselev, A. Lopatkin, Pham Quang Du, J. Chem. Soc. Faraday Trans. II 74 (1978) 367.
[43] A.G. Bezus, M. Kocirik, Collect. Czechoslov. Chem. Commun. 44 (1979) 660.
[44] A.V. Kiselev, Pham Quang Du, J. Chem. Soc. Faraday Trans. II 77 (1981) 1.
[45] S. Fritzsche, Phase Transitions 52 (1994) 169.
[46] P.I. Pohl, G.S. Heffelfinger, D.M. Smith, Mol. Phys. 89 (1996) 1725.
[47] S. Fritzsche, R. Haberlandt, J. Kärger, H. Pfeifer, K. Heinzinger, Chem. Phys. 174 (1993) 229.
[48] P. Denwontis, G.B. Suffritti, J. Phys. Chem. B 101 (1997) 5789.
[49] P. Demontis, G.B. Suffritti, Chem. Phys. Lett. 223 (1994) 355.
[50] S. Fritzsche, R. Haberlandt, J. Kärger, H. Pfeifer, M. Waldherr-Teschner, Studies in Surface Science and Catalysis, Vol. 84, Elsevier, Amsterdam, 1994, p. 2139.
[51] S. Fritzsche, R. Haberlandt, J. Kärger, H. Pfeifer, K. Heinzinger, M. Wolfsberg, Chem. Phys. Lett. 242 (1995) 361.
[52] General Discussion during the Faraday Symposium 26, Molecular Transport in Confined Regions and Membranes, J. Chem. Soc. Faraday Trans. 87 (1991) 1797.
[53] W. Heink, J. Kärger, S. Ernst, J. Weitkamp, Zeolites 14 (1994) 320.
[54] S. Fritzsche, R. Haberlandt, J. Kärger, Z. Phys. Chem. 189 (1995) 211.